

# Surface Roughness of Metallic Films Probed by Resistivity Measurements<sup>†</sup>

A. L. Cabrera,\* W. Garrido-Molina,<sup>‡</sup> E. Morales-Leal, and J. Espinosa-Gangas

Facultad de Física, Pontificia Universidad Católica de Chile, Casilla 306, Santiago 22, Chile

Ivan K. Schuller

Physics Department, University of California, San Diego, La Jolla, California 92093-0319

D. Lederman

Physics Department, West Virginia University, Morgantown, West Virginia 26506-6315

Received July 3, 1997. In Final Form: March 4, 1998

The resistance of thin cobalt (Co) and niobium (Nb) films was monitored during their exposure to hydrogen or carbon monoxide for 1000 s, at a fixed pressure, and also during the removal of the gas from the surface. In an adsorption–desorption cycle the resistivity changed in a “saw-tooth” fashion, similar to the changes observed in traditional gravimetric studies. The resistivity increase caused by the adsorbed gas seems to be directly related to weakly adsorbed states and the roughness of the film surface. The surface roughness decreases the magnitude of the adsorption-driven resistivity change in such a way that rough-thin Co films show a similar resistance change to that for smooth-thick Nb films. The roughness of the films depends on the deposition technique used, and it was determined by low-angle X-ray diffraction and scanning tunneling microscopy.

## Introduction

There are some issues related to gas adsorption by surfaces that have not been extensively studied yet. One of these issues is the connection between adsorption and its effect on the electrical conductivity of the substrate. In the case of strong adsorption of gaseous molecules by metallic surfaces, it is reasonable to expect a modification of the surface electrical conductivity of the metal. Thus, studying changes in the surface conductivity of the substrate produced by gas adsorption might yield additional information of the adsorption mechanism. Since the surface and bulk contribute to the total electrical conductivity of the substrate, surface conductivity only becomes dominant when the substrate's thickness is reduced to small values. Such is the case of thin films. Consequently, an effect due to adsorption on the surface conductivity would be more readily detectable in a thin film than in a metal foil or single crystal.

In particular, transition metals are excellent candidates for these studies because they adsorb H<sub>2</sub> and CO well. Most transition metals are good catalysts for the production of hydrocarbons from the reaction of H<sub>2</sub> with CO.<sup>1,2</sup> A necessary intermediate step for these reactions to take place is the adsorption and dissociation of both molecular H<sub>2</sub> and CO on the surface of the catalyst. In general, two hydrogen chemisorption states ( $\beta_1$  and  $\beta_2$ ) and a molecular

CO state and dissociated CO states are present on the surface of metals which adsorb these gases.

Nickel, cobalt, and iron adsorb hydrogen on the surface with almost no diffusion into the bulk<sup>3–10</sup>. The adsorption of hydrogen and CO on polycrystalline Ni and Co surfaces<sup>8–10</sup> and single-crystal Ni with different surface orientations<sup>3,11,12</sup> has been studied extensively. Thus the adsorption and desorption kinetics for these cases are well-known.

Shanabarger studied the adsorption of hydrogen on thin Ni<sup>13,14</sup> and Fe<sup>15</sup> films by monitoring their resistance during the exposure of the films to hydrogen. He found that the resistance of the films always increased when exposed to the gas, and from these data he was able to obtain the activation energy for adsorption. The low activation energies for desorption observed in his studies implied that the effect depended exclusively on the occupation of the  $\beta_1$  state. The fact that the resistance of the film is sensitive to this state of adsorption and not to the higher energy one ( $\beta_2$ ) suggests that this effect is not related to an electron-transfer mechanism.

Niobium allows some diffusion of hydrogen atoms<sup>16</sup> into subsurface sites (0.0028 atomic fraction). In this case,

<sup>†</sup> This article was originally submitted for the Bent Symposium issue (March 17, 1998).

\* To whom correspondence should be addressed.

<sup>‡</sup> Present address: Geodatos, S. A. I. C., Román Díaz 773, Santiago, Chile.

(1) Vannice, M. A. *J. Catal.* **1975**, *37*, 449.

(2) Somorjai, G. A. *Catal. Rev. Sci. Eng.* **1981**, *23*, 189.

(3) Russel, J. N., Jr.; Gates, S. M.; Yates, J. R., Jr. *J. Chem. Phys.* **1986**, *85*, 6792.

(4) Nyberg, C.; Westerlund, L.; Jonsson, L.; Andersson, S. *J. Electron Spectrosc. Relat. Phenom.* **1990**, *54/55*, 639.

(5) Norskov, J. K. *Rep. Prog. Phys.* **1990**, *53*, 1253.

(6) Burke, M. L.; Madix, R. *Surf. Sci.* **1990**, *237*, 20.

(7) Luengo, C. A.; Cabrera, A. L.; MacKay, H. B.; Maple, M. B. *J. Catal.* **1977**, *47*, 1.

(8) Cabrera, A. L. *J. Vac. Sci. Technol. A* **1990**, *8* (4), 3229.

(9) Cabrera, A. L. *J. Vac. Sci. Technol. A* **1993**, *11* (1), 205.

(10) Cabrera, A. L.; Garrido, W.; Volkman, U. G. *Catal. Lett.* **1994**, *25*, 115.

(11) Lapujoulade, J.; Neil, K. S. *C. R. Hebd. Seances. Acad. Sci.* **1972**, *C274*, 2125.

(12) Christmann, K.; Schober, O.; Ertl, G.; Neumann, M. *J. Chem. Phys.* **1974**, *60*, 4528.

(13) Shanabarger, M. R. *Solid State Comm.* **1974**, *14*, 1015.

(14) Shanabarger, M. R. *Surf. Sci.* **1974**, *44*, 297.

(15) Shanabarger, M. R. *Surf. Sci.* **1975**, *52*, 689.

(16) Pick, M. A. *Phys. Rev. B* **1981**, *24* (8), 4287.

resistance changes have also been observed upon the absorption of H.<sup>16,17</sup> The inhibition or enhancement of hydrogen absorption by metallic overlayers has also been observed in these types of experiments.<sup>18–20</sup> Pd, on the other hand, is the only metal which absorbs hydrogen into the bulk in large quantities:<sup>21</sup> two H atoms for every 4 Pd atoms in the lattice (0.33 atomic fraction). Several theoretical models have been developed to explain the large bulk diffusion of hydrogen into Pd and the absence of it into Nb and Ni.<sup>22–24</sup>

Other studies have claimed resistance increases due to surface adsorption of gases such as oxygen molecules on silver films.<sup>25,26</sup> Moreover, UPS measurements on the O/Ag and O<sub>2</sub>/Ag have shown that a  $\pi$  orbital of the adsorbed molecules was located above the Fermi level of the silver film, where conduction electrons can be additionally scattered.<sup>27</sup>

Several explanations have been advanced to explain changes in film resistance with adsorbed gas. The Suhrmann model<sup>28</sup> claimed that the molecular orbitals of a molecule located on the surface overlap with the conduction bands. The Sachtler model<sup>28</sup> hypothesized that there is an effective decrease in the thickness of the metal film when the molecules are adsorbed on the surface. A model based on the Fuchs–Sondheimer theory<sup>28</sup> is the most accepted model to explain these results. This model hypothesizes that the surface adsorbed molecules increase the resistance of the film because they increase the diffusive scattering of reflected electrons from the surface. This is assuming that the surface morphology of the film is perfectly planar. A refinement of this theory, known as “the scattering hypothesis”,<sup>28</sup> is a more general case. In this model, surface roughness is considered to give rise to a larger diffuse scattering, thus making the relative effect of the adsorbed molecules on the resistivity smaller.

In this paper, we studied the effect of H<sub>2</sub> or CO adsorption on the resistance of Co and Nb films. The film resistance increases monotonically with exposure to hydrogen or CO until saturation is reached when the surface is completely covered with molecules. This absolute resistivity change at saturation decreases with increasing film thickness. The most striking result is that the resistance change in a 200-nm sputter-deposited Co film exposed to 1000 L of CO is twice that for a 6-nm PVD-deposited Co film exposed to the same dosage of CO. These results point out that there is a connection between the change in resistance due to gas adsorption and the surface morphology of the films.

### Experimental Section

Thermal desorption and resistivity were measured for Co and Nb films exposed to H<sub>2</sub> and CO in a modified AMETEK (Thermox Instruments Division) system designed for gas analysis. The

(17) Kim, S.-W.; Sohn, K.-S. *Surf. Sci.* **1992**, *276*, 139.

(18) Pick, M. A.; Davenport, J. W.; Strongin, M.; Dienes, G. J. *Phys. Rev. Lett.* **1979**, *43*, 286.

(19) Strongin, M.; El-Batanouny, M.; Pick, M. A. *Phys. Rev. B* **1980**, *22*, 3126.

(20) Smith, R. J. *Phys. Rev. B* **1980**, *21*, 3131.

(21) Cabrera, A. L.; Morales, E.; Armor, J. N. *J. Mater. Res.* **1995**, *10*, 779.

(22) Davenport, J. W.; Dienes, G. J.; Johnson, R. A. *Phys. Rev. B* **1982**, *25*, 2165.

(23) Lagos, M.; Schuller, I. K. *Surf. Sci.* **1984**, *138*, L161.

(24) Rogan, J.; Lagos, M.; Schuller, I. K. *Surf. Sci.* **1994**, *318*, L1165.

(25) Schmiedl, E.; Watanabe, M.; Wissmann P.; Wittmann, E. Z. *Phys. Chem.* **1986**, *148*, 153.

(26) Wedler, G. *Adsorption and Reactions on Thin Metal Films in Thin Metal Films and Gas Chemisorption*; Wissmann, P., Ed.; Elsevier: Amsterdam, 1987; section 5.3, p 63.

(27) Barteau, M. A.; Madix, R. J. *Chem. Phys. Lett.* **1983**, *97*, 85.

(28) *Surface Physics*; Hohler, G., Ed.; Springer Tracts in Modern Physics No 77; Springer-Verlag: Berlin, 1975.

experimental chamber consists of a six-way stainless steel cross (base pressure in the low 10<sup>-9</sup> Torr) mounted on a pumping system, equipped with a sample manipulator, an Ar ion sputtering gun, a quadrupole mass spectrometer, a variable leak valve, and a glass viewport.

Gas evolution and resistivity measurements were performed on 40-, 200-, and 400-nm films of Nb ( $\approx 1.1 \times 0.3$  cm<sup>2</sup> area) and 200-nm films of Co ( $\approx 1.0 \times 1.0$  cm<sup>2</sup> area) sputtered onto sapphire substrates ((0 0 1) orientation). The same types of experiments were performed on 6-, 15-, or 30-nm films of Co ( $\approx 0.9 \times 1.2$  cm<sup>2</sup> area) evaporated (PVD) in UHV onto mica. The films were evaporated onto the basal planes ((0 0 1) orientation) of a piece of mica about 1-mm thick. Starting Co and Nb targets used for the films were 99.999% pure. Elemental surface composition was monitored with Auger electron spectroscopy (AES) or X-ray photoelectron spectroscopy (XPS) using a hemispherical analyzer (Physical Electronics, System 5100). Spectra in the 15–1000-eV energy range show typical surface C and O without any other impurity.

The crystal structure of the films was characterized with high- and low-angle X-ray diffraction (XRD) using a rotating anode X-ray diffractometer. XRD at low angle can be performed with the X-ray source and detector in a specular arrangement (if the angle between the X-ray source and the surface is  $\alpha$  and the angle between the detector and the surface is  $\beta$ , then  $\alpha = \beta = \theta$ ) or performed at off-specular angles ( $\alpha = \beta + 0.1^\circ$ ). The difference in XRD intensities between specular and off-specular arrangements gives some information about surface roughness.

Another way of obtaining information about the surface roughness is by performing XRD with the detector fixed in space and rotating the sample so that  $\alpha + \beta = 2\theta$  remains constant. The X-ray intensity pattern obtained in this way (as a function of  $\alpha - \beta$ ) is called the “rocking curve”.

Specular XRD taken at low angles confirmed that the estimated thicknesses for the films using a quartz thickness monitor during deposition were correct. The thicknesses obtained from XRD for the 15-nm Co film and the 40-nm Nb film were 15.4 and 41.4 nm, respectively.

Scanning tunneling microscopy (STM) inspection of the surface of the films was performed with a “walker” type of probe using RHK electronics, interfaced with a PC for image processing. The inspection was done using Pt–Rh tips electrochemically etched. More details of this system can be found elsewhere.<sup>29,30</sup>

Electrical contacts were provided for the films with a conductive emulsion of small metal particles in ethyl acetate (Loctite “Quick Grid”). Two insulated gold wires were connected to the film, at the location of the conductive paint on one side and spot welded to pins of a UHV feedthrough on the other side. The electrical resistance of this configuration was measured with a Keithley MicroOhmmeter (model 580) using the typical four-point probe method.

To clean the surface, the samples were subjected to two cycles of heating to 450 K followed by Ar ion sputtering. Ar ion sputtering was carried out on a  $1 \times 1$  cm<sup>2</sup> area with an ion current of 1  $\mu$ A for 2 min, which removed less than 1 nm of metal. Assuming the absence of contaminants after this process, the samples were exposed to 1000 L (1 L = 10<sup>-6</sup> Torr s) of hydrogen or CO at 320 K while the resistivity was measured. For each exposure, the cleaning cycle was repeated prior to the gas exposure.

### Results and Discussion

Representative X-ray diffraction (XRD) patterns were obtained for the Co and Nb films used in the adsorption experiments. High-angle scans between 20° and 100° showed the presence of a cubic fcc phase with (1 1 0) and (1 0 0) preferential orientations in the Co films. The Nb films are cubic bcc, all well textured along the (1 1 0) orientation.

(29) Somorjai, G. A. *Surface Chemistry and Catalysis*; John Wiley & Sons: New York, 1994; 392.

(30) Salmeron, M. *Studies of Chemisorption with the Scanning Tunneling Microscope*. In *Springer Proceeding in Physics*; Ponce, F. A., Cardona, M., Eds.; Springer-Verlag: Berlin, 1992; Vol. 62.

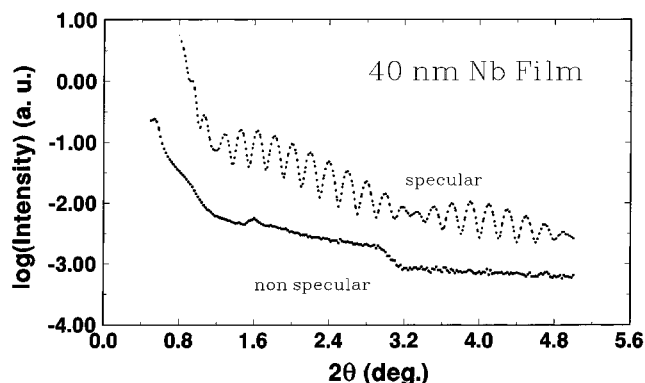


**Figure 1.** Longitudinal ( $\theta-2\theta$ ) X-ray reflectivity scan for the 40-nm Nb film. The peaks represent the interference between the top and bottom surface of the Nb film ("finite-size" peaks).

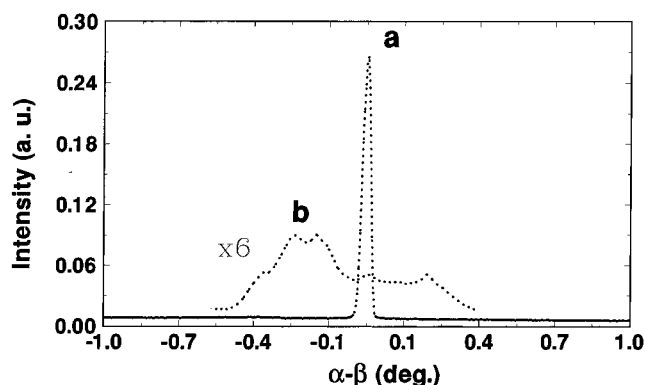


**Figure 2.** Representative X-ray diffraction curves ("rocking curves") obtained at low angle for (a) 40-nm Nb ( $2\theta = 1.28^\circ$ ) and (b) 15-nm Co films ( $2\theta = 1.20^\circ$ ).

Low-angle scans were taken between  $0.5^\circ$  and  $5.0^\circ$ . A typical curve obtained at low angle for the 40-nm Nb film is displayed in Figure 1. In this curve, the series of maxima and minima in the diffraction patterns are caused by the interference of scattered X-rays from the Nb surface and the Nb/sapphire interface. From this interference pattern it is possible to obtain an accurate thickness value for the film. In this case, the Nb film thickness corresponds to 41.4 nm. Similar diffraction patterns are obtained for the sputter-deposited Co films.

Low-angle scans were taken for the films in specular and off-specular arrangements. In the case of Nb films (the same for all sputter-deposited films), the intensity obtained in the specular arrangement is more than 15 times the intensity obtained in the off-specular arrangement, indicating a very smooth surface. In the case of the PVD-deposited Co films, there is no substantial intensity difference, indicating that the surfaces of these films are rough.

"Rocking curves" for the 40- and 400-nm Nb films and the 15-nm Co film were obtained ( $2\theta \approx 1.2^\circ$ ), and they are displayed in Figure 2. The "rocking curve" for the 400-nm Nb film is very similar to the curve obtained for the 40-nm Nb film, and therefore it is not shown in Figure 2. The "rocking curve" for the 40-nm Nb film (curve a) is well-defined and narrow. This film also exhibits a well-defined texture along the (110) orientation and a large ratio ( $\approx 15$ ) between specular and diffuse scattering. On the other hand, the "rocking curve" for the Co film (curve b) is very broad and has a smaller intensity, indicating that the Co film is much rougher than the Nb film. As will be pointed out later, this may explain a drastic difference observed in the resistivity change due to gas adsorption between sputter- and PVD-deposited films.

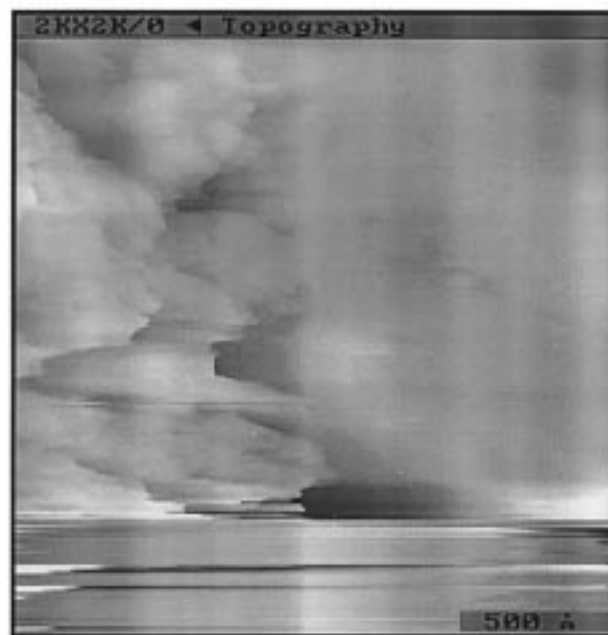


**Figure 3.** (a, top)  $300 \times 300 \text{ nm}^2$  STM image of the surface of a 15-nm PVD-deposited Co film (magnification  $\times 360\,000$ ). Corrugation is approximately 5 nm. (b, bottom)  $200 \times 200 \text{ nm}^2$  STM image of the surface of a 400-nm sputter-deposited Nb film at a similar magnification. No appreciable corrugation is seen.

These "rocking curves" performed at low angles characterize roughness at lateral length scales of the order of 50 nm (determined by the coherence length of the X-ray beam) to several thousand nanometers (determined by the projection of the X-ray beam on the sample's surface).<sup>31</sup>

Images of the surface of the 15-nm PVD-deposited Co film and the 400-nm sputter-deposited Nb film are displayed in Figure 3. The images were obtained scanning an area of  $300 \times 300 \text{ nm}^2$  for Co (Figure 3a) and  $200 \times 200 \text{ nm}^2$  for Nb (Figure 3b). Scans of  $300 \times 300 \text{ nm}^2$  correspond to a magnification of  $\times 360\,000$ . In this scale, which is comparable to roughness determined from XRD

(31) Fullerton, E. E.; Schuller, I. K.; van der Straeten, H.; Bruynseraede, Y. *Phys. Rev. B* **1992**, *45*, 9292.

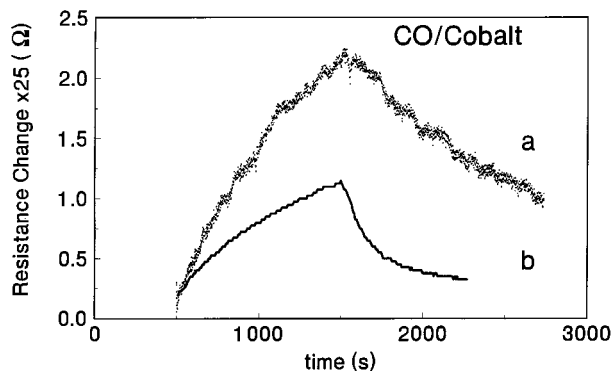


**Figure 4.** Resistance changes of Co films when exposed to CO for 1000 s and after removal of the gas: (a) 200-nm sputter-deposited film; (b) 6-nm PVD-deposited film.

**Table 1. Changes in the Resistance of Rough PVD-Made Co Films of Different Thicknesses Exposed to 1000 L of Carbon Monoxide at 335 K**

$N_i$ (nm)	$R$ ( $\Omega$ )	$\Delta R$ ( $\Omega$ )	$\Delta R/R(\times 100)$
06	4.10	0.040	0.98
15	2.05	0.010	0.49
30	0.82	0.002	0.24

**Table 2. Changes in the Resistance of Smooth Sputtered-Made Nb Films of Different Thicknesses When Exposed to 1000 L of Carbon Monoxide or Hydrogen at 335 K**

$N_i$ (nm)	$R$ ( $\Omega$ )	carbon monoxide		hydrogen	
		$\Delta R$ ( $\Omega$ )	$\Delta R/R(\times 100)$	$\Delta R$ ( $\Omega$ )	$\Delta R/R(\times 100)$
40	11.5	0.090	0.78	0.110	0.96
200	6.5	0.030	0.46	0.030	0.46
400	1.6	0.003	0.19	0.004	0.25

measurements, the Co surface appears to be covered with small clusters of about 5 nm in diameter. On the other hand, the Nb surface appears perfectly flat at the same magnification.

The resistivity of all Co and Nb films increased during exposure to hydrogen or CO (at 320 K) and decreased to approximately the initial value when the gas was removed from the chamber. These changes were quite reproducible and a "saw-tooth" pattern was obtained for cycles of adsorption/desorption on films of different thicknesses.

Figure 4 shows the resistance change of a 200-nm sputter-deposited Co film (curve a) and a 6-nm PVD-deposited (curve b) Co film upon exposure to CO. The films are exposed to CO for times between 500 and 1500 s in the graph. The gas is then turned off and pumped out of the chamber. When the gas is pumped out, the resistance decreases (times between 1500 and 2500 s).

One striking feature of this figure is that the resistance increase of a 200-nm sputter-deposited film under CO is almost twice as large as the resistance increase of the 6-nm PVD-deposited Co film under the same amount of CO dosage. We had expected to see a decrease in the resistance proportional to the ratio 6/200, since this surface effect decreases proportionally to the thickness of the film.

Results for the resistance change and relative resistivity change of various Co (PVD-deposited) films exposed to CO and various Nb (sputter-deposited) films exposed to H<sub>2</sub> and CO are displayed in Tables 1 and 2, respectively. For example, the resistance increase of the 6-nm Co film after 1000 L of CO exposure is approximately  $4 \times 10^{-2} \Omega$  (initial resistance is 4.10  $\Omega$ ). This corresponds to a relative resistivity change of 0.98%. The relative resistance change decreases to 0.49% for the 15-nm film and to 0.24% for the 30-nm film.

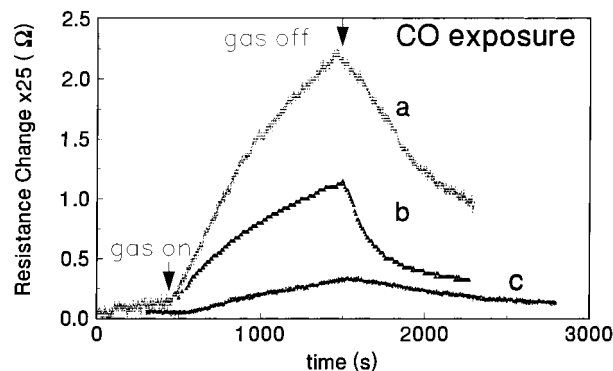


**Figure 5.** Resistance changes of Nb and Co films exposed to CO for 1000 s and after removal of the gas: (a) 40-nm Nb film; (b) 6-nm Co film for comparison; (c) 400-nm Nb film.

Figure 5 shows the resistance changes of a 40-nm (curve a) and 400-nm (curve c) sputter-deposited Nb film and the resistance change of the same 6-nm Co PVD-deposited film (curve b) when exposed to CO.

Resistivity changes of similar value for film thicknesses as different as those of Co PVD-deposited and Co sputter-deposited (or Nb sputter-deposited) films indicate that the surface resistance of the sputter-deposited films is more sensitive to modification by the adsorption of these gases than in the case of the PVD-deposited films. One way to explain this—which is consistent with the Fuchs–Sondheimer model—is that the surface quality of the sputter-deposited films is much better than that of the PVD-deposited films. Within the Fuchs–Sondheimer theory surface quality means that the fraction of conduction electrons scattered in the forward direction is much larger than the fraction scattered in the backward direction. This assumption is supported by our XRD and STM observations that the sputter-deposited films are definitely smoother than the PVD-deposited films.

The slight performance difference between Co and Nb sputter-deposited films in these experiments should be attributed to a difference in adsorption kinetics. The resistance curves during adsorption or desorption of the gases by the films carry important kinetic information as shown by Pick et al.<sup>16</sup> As will be shown later, Nb and Co curves can be fitted using the same parameter  $b$  which is proportional to the desorption energy, indicating that the kinetics of adsorption and desorption for both metals are very similar.<sup>32</sup>

It is well-known that the clean surface of metals such as Nb and Co is very reactive toward the dissociation of adsorbed molecules of CO and H<sub>2</sub>. So the question which comes to mind is: Which state of adsorption is responsible for the resistance increase?

Lauterbach et al.<sup>33</sup> have demonstrated, using Fourier transform infrared spectroscopy (FTIRAS), that the peak displayed at 378 K in a thermal desorption spectrum (TDS) of CO from a metal surface corresponds to *molecular* CO adsorption. This low-temperature desorption peak in a TDS indicates that molecular CO can be removed from the surface of Co and Nb at temperatures not much higher than room temperature. Moreover, the resistivity of the films at a temperature  $\approx 320$  K is readily altered by any variation in the CO partial pressure in the chamber.

Thus, we must assume that the occupation of the molecular-adsorbed CO state is responsible for the resistance change, since heating to higher temperatures is

(32) Papp, H. *Surf. Sci.* **1985**, *149*, 460.

(33) Lauterbach, J.; Wittmann, M.; Kupperts, J. *Surf. Sci.* **1992**, *279*, 287.

**Table 3. Curve Fitting Using Eq 3.1 for the Nb and Co Films' Resistance Increase When Exposed to Hydrogen or Carbon Monoxide at 335 K<sup>a</sup>**

$N_f$ (nm)	metal	carbon monoxide		hydrogen	
		$a$	$a^*$	$a$	$a^*$
006	Co PVD	0.0014	0.0225		
200	Co sputter	0.0026	0.0007		
040	Nb sputter	0.0026	0.0049	0.0044	0.0049
200	Nb sputter	0.0014	0.0010		
400	Nb sputter	0.0005	0.0005		

<sup>a</sup> The parameter  $b$  is around 3 for all the curves. The parameter  $a^*$  was calculated from eq 3.4 assuming  $s_0/x_{\max} = 1$ .

always required to remove dissociated CO from the surface. A small resistance change in the films due to the dissociated CO on the surface can explain the fact that the resistance never comes back to the initial value when the gas is removed from the chamber without heating the sample.

The resistance change in the Nb films caused by the H<sub>2</sub> desorption is related to the occupation of the  $\beta_1$  state (a weakly adsorbed state), since heating the films is not normally required to remove the gas from the surface. The occupation of the  $\beta_2$  state is responsible for the small resistance difference from the initial value after the H<sub>2</sub> is removed from the chamber. These results strongly suggest a connection between surface resistivity changes and the occupation of weakly adsorbed molecules on the film surfaces.

Since the resistance change of Nb films due to H<sub>2</sub> adsorption is similar to the change observed during CO adsorption, we can safely assume that the films did not absorb substantial amounts of hydrogen during our experiments. Our results strongly support the idea that the resistance increase of the films when exposed to gases is due to a surface resistance increase. The surface resistance change due to gas adsorption is an effect that decreases with the thickness of the films and disappears for thick films (see Tables 1 and 2).

The changes in resistance of the Co and Nb films caused by the adsorption or desorption of hydrogen and CO in the present studies are similar to those observed in other experiments<sup>16,18</sup> which involved thin Nb foils exposed to hydrogen. It was claimed in that work that the Nb foils absorbed some hydrogen in the bulk (0.0028 atomic %). Nb or any other metal definitely does not absorb CO into the bulk (except for subsurface carbon or oxygen as a result of dissociation of the CO molecule).

A kinetic analysis of the adsorption/absorption process done by Pick et al.<sup>16</sup> allowed them to develop an analytical expression for the resistance increase during adsorption and for the resistance decrease during desorption. The model considered four fluxes of gas at the surface/bulk interface:  $f_1$ , a flux impinging on the surface (adsorption);  $f_2$ , a flux leaving the surface (surface desorption);  $f_3$ , a flux diffusing from the surface into the bulk (absorption); and finally,  $f_4$ , a flux diffusing from the bulk to the surface (bulk desorption). Using this model, the resistance increase can be fitted with the following analytical expression:

$$(1 - b)^2 \ln(1 + y) - (1 + b)^2 \ln(1 - y) - 2b^2 y = 2at \quad (3.1)$$

where  $y$  can be the normalized resistance change ( $y = \Delta R/\Delta R_{\max}$ ),  $t$  is time, and  $a$  and  $b$  are fitting parameters.

In our case, the fluxes  $f_3$  and  $f_4$  are negligible compared to  $f_1$  and  $f_2$ , since there is no diffusion of gas into the bulk. This is taken into account in the model, and the resistance

increase curves for Nb for hydrogen exposure (not shown) and CO exposure (Figure 5) and for Co for CO exposure (Figure 4) are reasonably well fitted with eq 3.1. The parameters  $a$  and  $b$  obtained for the fit are listed in Table 3.

The parameter  $b$  is given by the following equation:

$$b = (\beta/\nu)x_{\max} \quad (3.2)$$

where  $\nu$  is the diffusion constant (with activation energy  $E_A$ ) for gas entering the bulk of the film (flux  $f_3$ ) and  $\beta$  is the diffusion constant (with activation energy  $E_B$ ) for gas leaving the bulk (flux  $f_4$ ). The energies of all of these activation barriers satisfy the equation

$$E_B - E_A = E_s - E_d \quad (3.3)$$

The fraction  $\beta/\nu$  is proportional to  $\exp -(E_s - E_d)/RT$  (from eq 3.3). This fraction must be large, since  $x_{\max}$  must be very small (specially for CO because neither of the films absorb CO) in order to obtain the product of these two quantities equal to 3.

$\ln(b)$  is proportional to the solution energy ( $E_s$ ) required for the gas to dissolve into the bulk and proportional to the surface chemisorption energy ( $E_d$ ). To obtain accurate values for the desorption energy, the solution energy or the absolute amount of gas dissolved into the bulk (even if it is very small) must be determined by an independent measurement. Since we have not determined either one in our experiments, we are giving only relative values for  $a$  and  $b$ .

According to the same reference,<sup>18</sup>  $a$  can also be related to the flux of molecules ( $\Gamma$ ) impinging upon the film surface, the initial sticking coefficient ( $s_0$ ), the number of surface atoms ( $N_s$ ) of the film, the thickness ( $N_f$ ) of the film, and the maximum atomic fraction of gas dissolved ( $x_{\max}$ ):

$$a = 2\Gamma s_0/N_s N_f x_{\max} \quad (3.4)$$

For our conditions:  $\Gamma = 1.35 \times 10^{15}$  molecules/(cm<sup>2</sup> × s), since we keep the pressure and the temperature constant. Using the program Surface Architecture and Latuse<sup>34</sup> we can estimate the lattice spacing and number of surface atoms for bcc Nb (1 1 0) and fcc Co (1 1 0). The Nb lattice spacing is 0.234 nm, and that for Co is 0.125 nm. This implies that there are about 48 layers in 6 nm of Co, 1600 layers in 200 nm of Co, 171 layers in 40 nm of Nb, 855 layers in 200 nm of Nb, and so forth. Finally, assuming that adsorption only occurs on the very top layer,  $N_s$  is  $3.2 \times 10^{15}$  atoms/cm<sup>2</sup> for Nb and  $2.5 \times 10^{15}$  atoms/cm<sup>2</sup> for Co. Using these values and assuming that  $s_0/x_{\max} = 1$  for both cases, we can calculate a theoretical value for  $a$ . This is denoted as  $a^*$  and also listed in Table 3. Since we do not know the value of  $x_{\max}$  or  $s_0$ , we have chosen a value of 1 for their fraction in order to see how  $a^*$  changes as a function of thickness. The value chosen is such that  $a^*$  is not too different from the fitted value of  $a$  for the 400-nm Nb film.

Assuming that the initial sticking coefficient  $s_0$  for the adsorption of CO is similar for both types of Co films, then the  $a$  parameter for the 6-nm PVD-deposited Co film should be 33 times larger than that for the 200-nm sputter-deposited Co film (based purely on a kinetic effect, disregarding surface morphology). Looking at Table 3, we find the opposite; the  $a$  for 200-nm sputter-deposited Co film is about 1.85 times larger than that for 6-nm PVD-

(34) Van Hove, M. A.; Hermann, K. Surface Architecture and Latuse, A PC-based Program, Version 2.0, Lawrence Berkeley National Lab., Berkeley, CA, 1988.

deposited Co. To compensate for this effect, we must assume that the number of Co surface atoms exposed to the gas is  $33 \times 1.85$  times larger for the PVD-deposited film than that for the sputter-deposited film. This implies that the sputter-deposited films have less surface roughness than the PVD-deposited films.

This is additional support for our interpretation, which states that the change in resistance of the films caused by the surface adsorbed molecules strongly depends on the film's surface morphology. Differences in surface morphology are certainly present and supported by XRD and STM characterization of the films.

The changes in the resistance of the films have been claimed to be enhanced if the film smoothness increases.<sup>26,35</sup> Nowadays, the "scattering hypothesis"<sup>22</sup> is the most accepted model to explain these results. Within this model, surface roughness affects the total film resistance and thus adsorbed molecules only increase the fraction of scattering centers on the surface, which in turn cause diffuse scattering of conduction electrons. The effect of adsorbed molecules on film resistance would then be less pronounced for rough films than for smooth films, in agreement with our results.

The main issue remaining is related to the length scales of the roughness. The adsorption/desorption of hydrogen or CO as sensed by resistivity measurements is possibly affected in a first order manner by the simple increase in the surface area of the films. This is directly related to the low-angle X-ray diffraction measurements that were done to the films. Low-angle X-ray diffraction detects roughness at a length scale of 50 nm, which is larger than atomic length scales. Other researchers<sup>36,37</sup> found related

(35) Luo, E. Z.; Heun, S.; Kennedy, M.; Wollschlager, J.; Henzler, M. *Phys. Rev. B* **1994**, *49*, 4858.

(36) Holzapfel, C.; Akemann, W.; Schumacher, D.; Otto, A. *Surf. Sci.* **1990**, *227* 123.

(37) Hein, M.; Schumacher, D. *J. Phys. D: Appl. Phys.* **1995**, *28* 1937.

surface roughness at length scales of 1–10  $\mu\text{m}$  with changes in the resistivity of gas-covered silver films using visible and infrared radiation (wavelength between 23  $\mu\text{m}$  and 136 nm). All these results point out that there is definitely a connection between surface roughness at mesoscale and the resistivity increase due to the gas-covered surface.

The short atomic scale roughness is difficult to determine quantitatively for a surface of arbitrary roughness. In some limiting cases—such as flat surfaces with atomic scale steps—scanning tunneling microscopy can give excellent local atomic resolution. However, the resistivity increase observed in our films when they are covered with gas reflects the average of the overall roughness present at atomic and mesoscale on a macrosurface. The averaging of roughness at all length scales in scanning probe measurements is limited by the convolution of the tip shape with roughness, which is difficult to determine. On the other hand, the roughness determined by diffraction measurements is limited by the lateral coherence length of the radiation, which is well-known.

In any case, the present results confirm again the connection between surface roughness and resistivity change due to the adsorption of gases in metallic films.

**Acknowledgment.** Fundacion Andes is gratefully acknowledged for grant C-12776. This research was also supported by the Chilean Government (Fondecyt 1971215), P. Universidad Católica through DIPUC, and the U.S. National Science Foundation (NSF). Thanks are due to Prof. Gabor A. Somorjai, Dr. Miquel Salmeron, Mark Rose, and Nikos Jager, University of California, Berkeley, for making feasible the STM implementation in our laboratory.

LA970714W